Electrical conduction in homoepitaxial, boron-doped diamond films

1992 J. Phys.: Condens. Matter 4 7365

(http://iopscience.iop.org/0953-8984/4/36/011)

J. Phys.: Condens. Matter 4 (1992) 7365–7376. Printed in the UK

Electrical conduction in homoepitaxial, boron-doped diamond films

Eric P Visser, G J Bauhuis, Ger Janssen, W Vollenberg, Willem J P van Enckevort and L J Giling

Experimental Solid State Physics, University of Nijmegen, Faculty of Science, Toernooiveld, 6525 ED, Nijmegen, The Netherlands

Received 14 May 1992

Abstract. Epitaxial, boron-doped diamond films were grown by hot-filament-assisted chemical vapour deposition (CVD) on {100} and {110} natural diamond substrates. Resistivity measurements for $10\,K < T < 500\,K$ showed a clear transition from band to hopping conduction upon lowering of temperature. In the band conduction regime, the {100} films had higher conductivity than the {110} samples. The reverse was found in the hopping regime. This is explained by the difference in crystal growth mechanisms, leading to higher boron concentrations and lower carrier mobilities for {110} samples than for {100} oriented films. Hall effect measurements were performed for the most lightly doped (100) film at a boron level of 2.7×10^{18} cm^{-3} in the band conduction region up to 750K. A mobility maximum of $\mu_H = 590\,cm^2V^{-1}s^{-1}$ at 295K was found, and the compensation ratio was determined to be smaller than 0.02. Some preliminary values for the Hall effective mass of valence band holes are given.

1. Introduction

Electrical conduction in chemical-vapour-deposited (CVD) diamond films has been studied rather extensively. Most studies have been done for polycrystalline layers, both boron-doped and undoped, grown on non-diamond substrates. In this case, the interpretation of results is complicated by the presence of grain boundaries. For instance, activation energies higher than the boron ionization energy (typically between 0.7 and 1.0 eV [1–2], and even 2.3 eV [3]) have been observed in polycrystalline films. These high values, which to our knowledge have never been found for monocrystalline diamond, have been attributed to the presence of non-diamond carbon material at grain boundaries. Also, polycrystalline boron-doped films have shown much higher resistivity than homoepitaxial ones (compare, e.g., [4] and [5]). This effect is obviously due to carrier scattering at grain boundaries, and, in addition, it has been attributed to boron deactivation by clustering [6].

As far as we know, the only reports on electrical measurements of CVD-grown, homoepitaxial diamond films are [5], [7] and [8]. In these studies, the diamond films have been grown by microwave-plasma-assisted CVD and have been doped with boron from a B_2H_6 gas source, leading to p-type conductivity. The substrates used were type Ia natural diamond [8] and high-pressure/high-temperature- (HPHT-) grown synthetic diamond [5,7]. The lowest room temperature resistivity reported is $\approx 3 \times 10^{-3}\,\Omega$ cm at a boron concentration of 3×10^{20} cm^{-3} [5]. In this film, metallic

0953-8984/92/367365+12$04.50

conduction has been observed for the temperature region 300 K $< T <$ 770 K. The highest room temperature Hall mobility observed was 470 $cm^2V^{-1}s^{-1}$ with a carrier concentration of 2.2×10^{14} cm^{-3} [7]. Some doubt could exist, however, since the value of 310 $cm^2V^{-1}s^{-1}$ is also given for the same film (table III in [7]).

2. Experiments

The diamond films were grown in a conventional hot-filament-assisted CVD reactor using a gas mixture of 0.67% CH_4 in H_2 at 50 mbar with a flow rate of 0.3 standard litres per minute. The deposition time was 6 h. The substrates used were natural, type IIa, polished diamond plates of {100} and {110} orientation and resistivity $> 10^{16}\,\Omega$ cm. The filament temperature was 1910 °C. Boron doping was achieved by heating the hexagonal BN substrate holder, which led to outdiffusion of boron into the gas phase. The boron content of the diamond films could be controlled by adjusting the temperature of the substrate holder. Eight samples, grown in four different runs (each containing a (100) and a (110) sample) with temperatures between 735 °C and 915 °C, were investigated.

The films have already been characterized using optical spectroscopy and surface microtopography [9]. The room temperature neutral boron concentration N_A^0 ($= N_A - N_D - p$), as determined by infrared absorption [9], was found to vary between 2.7×10^{18} and 510×10^{18} cm^{-3}. An overview of layer thicknesses d and concentrations N_A^0 is given in table 1. It is seen that both the growth rates and the neutral boron concentrations are higher for {110} films than for {100} ones from the same run.

Table 1. Layer thickness d and neutral boron concentration N_A^0 at room temperature for eight homoepitaxial diamond films, grown in four runs (numbered HF-1, HF-2, HF-3 and HF-5, as in [9]). All boron concentrations were determined using the infrared absorption of the one-phonon band (see [9] for further discussion). The error in layer thickness is 5–10%. At small concentrations, the errors in N_A^0 are mainly caused by the overlap of the weak one-phonon absorption with the interference pattern in the infrared absorption spectrum. For high concentrations, the one-phonon absorption merges with the broad-band acceptor transition, which is then the main source of error.

Sample	d (μm)	N_A^0 (10^{18} cm^{-3})
HF-3(100)	1.5	2.7 ± 0.7
HF-2(100)	1.2	5.7 ± 2.8
HF-1(100)	0.9	19 ± 5
HF-5(100)	2.1	59 ± 6
HF-3(110)	7.4	18 ± 2
HF-2(110)	5.2	15 ± 4
HF-1(110)	3.9	47 ± 3
HF-5(110)	5.7	510 ± 130

Electrical conductivity measurements using the van der Pauw configuration were done for 10 K $< T <$ 500 K in a liquid-He-flow cryostat. The minimum temperature that could actually be used for each sample was limited by the film resistivity and the signal-to-noise ratio of the measurement equipment. For the layer thicknesses and lateral dimensions (typically 3–4 mm) of the samples investigated, the practical

resistivity limit was of the order of $10^5\,\Omega$ cm. This led to lower limits in temperature ranging from ≈ 10 K for the most heavily doped sample HF-5(110) to ≈ 100 K for the lightly doped ones. The settings of the current source ranged from $1\,\mu$A to 10 mA, at the corresponding voltages from 1 mV to 100 mV.

The metal contacts, consisting of sputtered Ti/Pt/Au layers, showed ohmic behaviour in all cases. The contact size was kept as small as possible (typically some tenths of a millimetre) and was in the worst case 20% of the distance between the contacts. Such a finite contact size could lead to systematic errors in the conductivity values of at most 10% [10]. In view of the uncertainty in layer thickness, the total systematic error in conductivity could be $\approx 15\%$.

Carrier concentrations and mobilities were determined by Hall effect measurements at $B = 0.6$ T for the most lightly doped sample HF-3(100) in the temperature range $230\,\mathrm{K} < T < 750\,\mathrm{K}$. For increased accuracy, this sample was laser-cut into a clover-leaf shape and again the van der Pauw configuration of contacts was used.

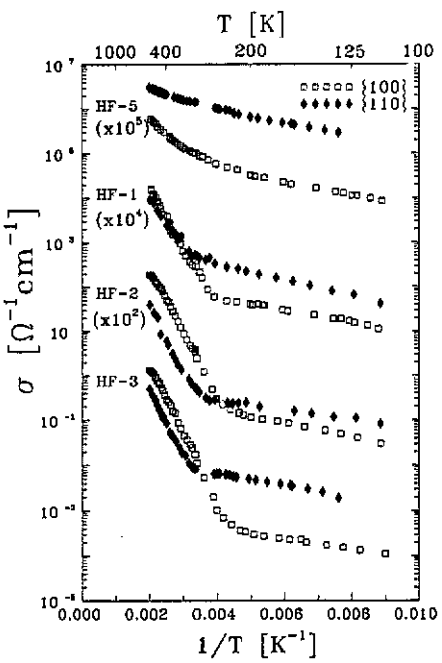

Figure 1. Conductivity of homoepitaxial diamond films of {100} and {110} orientation as a function of temperature. For a clear presentation of the data, the plots of runs HF-2, HF-1 and HF-5 have been shifted by the values indicated.

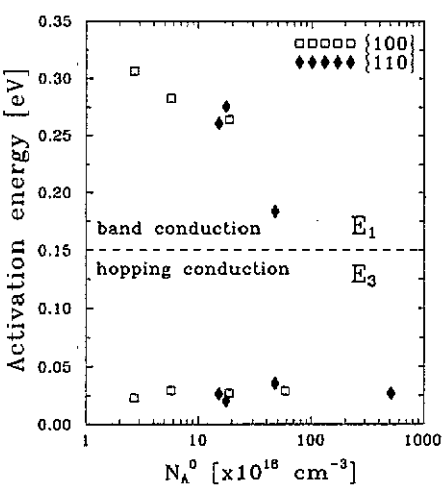

Figure 2. Activation energies for the band conduction region (E_1) and the hopping region (E_3) as a function of the room temperature neutral boron concentration N_A^0.

3. Experimental results

The results of the conductivity measurements for $110\,\mathrm{K} < T < 500\,\mathrm{K}$ are shown in figure 1. Except for the most heavily doped samples of the run HF-5, a clear difference in activation energy between high- and low-temperature regions can be

noted. Depending on the dopant content and crystallographic orientation, the transition occurs at temperatures between 225 and 310 K. In figure 1, the presented data are limited to temperatures > 110 K. The lower-temperature data, which are available for the samples of runs HF-1 and HF-5, will be given in figure 7 and discussed in section 4.3.

In view of the different activation energies, it is natural to consider two conduction mechanisms and accordingly express the conductivity σ as

$$\sigma = \sigma_1 e^{-E_1/kT} + \sigma_3 e^{-E_3/kT} \tag{1}$$

with $E_3 < E_1$ (the subscript 3 has been chosen in accordance with [11]). Such sharp transitions in activation energy upon lowering of temperature have been observed in other semiconductors [12, 13] and have been attributed to the change from band to hopping conduction. In the next section this will be discussed further; we shall be using the terms 'hopping conduction' and 'band conduction' for the low- and high-temperature regimes, respectively.

The energies E_1 and E_3 were determined by exponential fits to the data of figure 1 in both temperature regions. For the heavily doped samples (run HF-5), where no clear transition temperature was observed, only E_3 was calculated for the interval starting at $T = 220$ K down to the lowest data point in the figure. The results are shown in figure 2.

The carrier concentration p for the most lightly doped sample HF-3(100) at temperatures 230 K < T < 750 K is shown in the lower part of figure 3. The experimental values are indicated by squares. Two additional plots of the same data set, shifted by constant vertical distances, have been added in the figure. This was done in order to obtain a clear presentation of the theoretical fit curves which will be explained in section 4. The room temperature carrier concentration is $p(293\ \text{K}) = 1.32 \times 10^{14}\,\text{cm}^{-3}$. In calculating p from the measured Hall coefficient, $R_H = r/pe$, the Hall factor r was assumed to be unity.

The temperature dependence of the Hall mobility μ_H, calculated through $\sigma = pe\mu_H$, is shown in figure 4. The maximum value of $590\,\text{cm}^2\text{V}^{-1}\text{s}^{-1}$ is found at $T = 295$ K. Assumption of a power law $\mu \sim T^\kappa$, where κ is the mobility index, yields $\kappa_{low} = 2.2$ and $\kappa_{high} = -2.8$ for the low- and high-temperature limit, respectively.

4. Discussion

4.1. Band conduction

The normal conduction mechanism in a p-type semiconductor is the motion of valence band holes thermally excited from one or more acceptor levels. If a single level with ionization energy E_A is present, the activation energy E_1 (i.e. the slope of the $\ln p$ versus $1/T$ plot) is of the order of magnitude of E_A. In general, E_1 will be somewhat smaller than E_A, the exact value being dependent on the acceptor concentration, the compensation ratio and the temperature region (equation (2), section 4.1.1). Taking the reported value of $E_A = 0.3685$ eV for boron in diamond [14], the values of E_1 in figure 2 are as expected for conduction by valence band holes, excited from the boron acceptor level. It should be noted that we determined the activation energies using the conductivity data instead of the carrier concentration $p(T)$. However, since

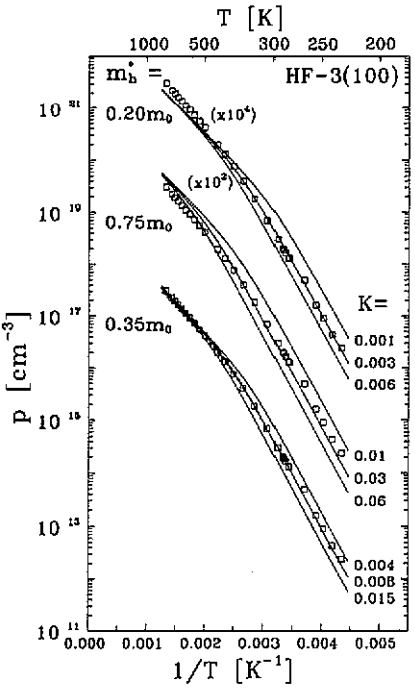

Figure 3. Carrier concentration p obtained from Hall measurements, as a function of temperature for sample HF-3(100) ($N_A^0 = 2.7 \times 10^{18}\,\mathrm{cm}^{-3}$). The experimental values are indicated by squares; the lines correspond to theoretical fits where the compensation ratio K and the Hall effective mass m_h^* have been varied (see section 4). For clarity of presentation, the values of p in the two upper graphs (which display the same data set as the lower one) have been multiplied by the factors indicated.

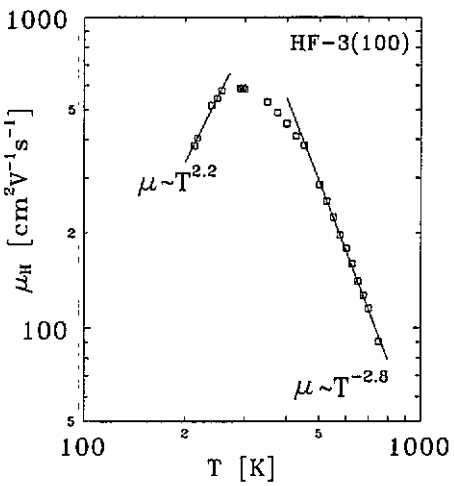

Figure 4. Temperature dependence of the Hall mobility μ_H for sample HF-3(100) ($N_A^0 = 2.7 \times 10^{18}\,\mathrm{cm}^{-3}$). The maximum value of $590\,\mathrm{cm}^2\mathrm{V}^{-1}\mathrm{s}^{-1}$ is found at $T = 295\,\mathrm{K}$. The high- and low-temperature data can be fitted using a power law $\mu \sim T^{\kappa}$. The resulting values of κ are $\kappa_{low} = 2.2$ and $\kappa_{high} = -2.8$.

the carrier mobility is generally much less dependent on temperature than p, the resulting values of E_1 will not differ much.

For the most heavily doped samples of run HF-5, the small activation energies in the high-temperature region (see figure 1) may indicate that metallic conduction is also present to some extent. Metallic conduction will be dominating for dopant concentrations above the Mott transition, given by $N_A a_h^3 \approx 0.02$ [16], where a_h is the Bohr radius for holes in diamond. Taking the value of $a_h = 0.403\,\mathrm{nm}$ (obtained for a hole effective mass of $m_h^* = 0.75 m_0$, m_0 being the electron rest mass), the semiconductor-to-metal transition should occur for $N_A = 3.1 \times 10^{20}\,\mathrm{cm}^{-3}$. The dopant concentration of the (110) film of run HF-5 is clearly above this value (see table 1).

4.1.1. Hall effective mass and compensation ratio. The temperature dependence of the carrier concentration (measured for sample HF-3(100) at $230\,\mathrm{K} < T < 750\,\mathrm{K}$, see figure 3) can be used to determine the compensation ratio $K \equiv N_D/N_A$. Theoretically, in a non-degenerate p-type semiconductor with a single acceptor level with ionization energy E_A and compensating deep donors at a concentration $N_D = KN_A$, the carrier concentration p is given by [15]

$$\frac{p(p+KN_A)}{(1-K)N_A-p}=\left(\frac{2\pi m_h^* kT}{h^2}\right)^{3/2} e^{-E_A/kT}. \quad (2)$$

The degeneracy factor g_A has been set equal to 2, which is the case for boron in diamond [17]. Furthermore, it is implicitly assumed that a single, scalar effective mass m_h^* can be used. Diamond has three valence bands, characterized by different effective-mass tensors. Therefore, m_h^* is the weighted average of the contribution of the three bands in the scalar approximation. Moreover, since p was determined using the Hall effect, in principle three different Hall factors r should be used for scattering of light and heavy holes and 'split-off' holes. By setting r equal to 1, this effect has been neglected. Therefore, the value of m_h^* is the average Hall effective mass, which could vary with magnetic field strength, temperature or crystal quality.

The experimental carrier concentrations of figure 3 were fitted by variation of the compensation ratio K and the effective mass m_h^* using the theoretical relation of equation (2). For the acceptor ionization energy, the fixed value of $E_A = 0.3685\,\text{eV}$ [14] was taken. For N_A, the relation $N_A = (N_A^0 + p)/(1-K)$ was used, where $N_A^0 = 2.7\times10^{18}\,\text{cm}^{-3}$ (the room temperature value of p can be neglected compared to N_A^0). It is seen in figure 3 that the effect of variation of K is most strongly felt at low temperatures, whereas the high-temperature values of p are mainly determined by m_h^*.

A very large scatter exists in the literature with regard to the hole effective mass for diamond. Values between $0.25m_0$ and $2.1m_0$ have been reported [18]. Often the value of $m_h^* = 0.75m_0$ is used. However, as is clear from figure 3, it is not possible to obtain a proper fit to the experimental data using $m_h^* = 0.75m_0$. The resulting carrier concentration would always be too high in the high-temperature region, independently of the chosen value for K. The best result was obtained using $m_h^* = (0.35\pm0.05)m_0$ and $K = 0.008\pm0.002$, as is shown in the lowermost curves. Choosing a still lower value of m_h^*, as shown in the upper curves, yields too low values of p at high temperatures. It should be mentioned that the error in the value of N_A^0 (see table 1) has little importance for the curve fitting. In the lower figure, two additional dashed curves have been drawn corresponding to $N_A^0 = 2.0\times10^{18}$ and $3.4\times10^{18}\,\text{cm}^{-3}$ at the same value of K and m_h^*. The dashed curves are hardly distinguishable from the solid one. Only in the high-temperature region is a very small deviation from the curve with $N_A^0 = 2.7\times10^{18}\text{cm}^{-3}$ noticed.

The resulting value of K leads to a concentration of deep donors, such as nitrogen, smaller than $2.2\times10^{16}\,\text{cm}^{-3}$. This is indicative of a very ineffective incorporation of nitrogen, which was also observed for flame-grown CVD diamond [19].

Finally, it should be noted (as has been explained in [9]) that a discrepancy exists between neutral boron concentrations based on calculations using two different infrared absorption bands. The value of $N_A^0 = (2.7\pm0.7)\times10^{18}\,\text{cm}^{-3}$ should be replaced by $(1.1\pm0.2)\times10^{18}\,\text{cm}^{-3}$ when the alternative method is used. This problem has not been solved yet and we refer the reader to [9] for a discussion. However, when the experimental carrier concentration is fitted using $N_A^0 = (1.1\pm0.2)\times10^{18}\,\text{cm}^{-3}$, the values of m_h^* and K obtained differ from those given above. We obtained $m_h^* = (0.65\pm0.05)m_0$ and $K = 0.020\pm0.003$. It is seen that a definite, reliable value for m_h^* cannot be given before the neutral boron concentration is known more accurately. On the other hand, the compensation ratio is still found to be low, also when the alternative value of N_A^0 is used in the fitting procedure.

From the above, it is clear that the value presented for the hole effective mass should be considered as preliminary. The Hall effect measurements have to be extended to more samples and unambiguous values for the boron concentration should be available. These could be obtained by using higher temperatures where the hole concentration approaches saturation. At the moment, however, we cannot handle the required temperatures, which are typically 1200 K or higher.

4.1.2. Hall mobility. The maximum Hall mobility of $590\,cm^2V^{-1}s^{-1}$ at 295 K (see figure 4) is the highest value reported for CVD-grown diamond. Higher values (up to $2000\,cm^2V^{-1}s^{-1}$) have been reported for natural and HPHT-grown synthetic diamond (for an overview, see, e.g., [8]). However, the dopant content of these samples was considerably lower than that of our films. We feel that the currently observed high value of μ_H should be attributed to the low degree of compensation and the good crystalline quality.

The values of $\kappa_{low} = 2.2$ and $\kappa_{high} = -2.8$ for the low- and high-temperature mobility index deviate from the theoretical values for impurity scattering (resulting in $\kappa_{low} = 1.5$) and lattice scattering (leading to $\kappa_{high} = -1.5$). This indicates that both at low and at high temperatures, scattering mechanisms other than the above-mentioned ones are effective. The observed value of $\kappa_{high} = -2.8$ is within the range of values given in [7] and [20].

4.2. Hopping conduction

Hopping conduction in semiconductors has been extensively studied (for a general treatment, see [11]). It is observed in the temperature region where band carriers have been frozen out and at dopant concentrations below the Mott transition. Furthermore, since hopping occurs between neutral and ionized dopant atoms, a certain degree of compensation is required.

In a typical semiconductor such as germanium, hopping conduction is only observed at very low temperatures (below 10 K [12]). In p-type diamond, however, where the acceptor ionization energy equals 0.37 eV, free holes will be virtually frozen out already at much higher temperatures. Furthermore, due to the small Bohr radius, metallic conduction only starts at acceptor concentrations exceeding $10^{20}\,cm^{-3}$. Therefore, hopping conductivity in p-type diamond can be studied in quite a large range of temperatures and dopant concentrations.

Experimental studies on hopping conduction have been carried out for HPHT-grown diamond [21,22]. For CVD diamond films, hopping conduction has only been studied in polycrystalline material [6], where boron clustering at grain boundaries has led to deviations from the expected values of σ_3 and E_3. For the measurements on homoepitaxial films mentioned in the introduction [5,7,8], no low-temperature data have been reported and accordingly transitions between band and hopping conduction have not been observed.

In section 3, we have already attributed the transition between high and low activation energies to a change from band to hopping conduction. This deserves some further discussion, however. A small activation energy does not necessarily imply E_3 conduction. Indeed, for n-type germanium, an additional term $\sigma_2 e^{-E_2/kT}$, describing the motion of electrons over singly filled neutral donors (occurring through the D^- state), has been added to equation (1) [23]. (For a discussion of this type of conduction, see [11].) In summary, the characteristics are: (i) the activation energy lies between E_1 and E_3; (ii) it occurs at intermediate temperatures between the

hopping region and the band conduction region; and (iii) it is only observed when the impurity concentration is high and the compensation ratio is low. For the moment, we cannot exclude the occurrence of E_2 conduction in the present diamond films.

A proof of the occurrence of hopping conduction could be given by the temperature dependence of the Hall coefficient R_H. It should go through a maximum at the transition from band to hopping conduction [12]. However, we were not able to measure the Hall coefficient in the hopping region using the present DC method. Most likely, an alternating magnetic field, such as in [24], should be used. The absence of a DC Hall effect in the hopping region has been found for several other materials [25].

On the other hand, the occurrence of hopping conduction can be verified by the dependence of the pre-exponential factor, σ_3, on the dopant concentration N_A. For band conduction, the conductivity should increase more or less linearly with N_A (in fact sublinearly, since the carrier mobility decreases at increasing dopant concentrations). In the hopping region, however, the conductivity is determined by the amount of impurity wave function overlap, which decays exponentially with the mean separation between dopant atoms, $(\frac{4}{3}\pi N_A)^{-1/3}$. Accordingly, σ_3 should obey a relation of the form

$$\sigma_3 = \sigma_{3,0} \exp\left[-\alpha \frac{N_A^{-1/3}}{a_h}\right] \tag{3}$$

where the theoretical value of α depends on the specific model used. For the Miller–Abrahams random resistor network and isotropic impurity wave functions, a value of $\alpha = 1.73$ is calculated [26]. Figure 5 shows the experimental conductivity data in the hopping region down to $T = 110$ K, together with the linear fits of ln σ versus $1/T$. The corresponding pre-exponential factors σ_3 are shown in figure 6 as a function of $(N_A^0)^{-1/3}$. Roughly speaking, an exponential dependence of σ_3 on $(N_A^0)^{-1/3}$ can be discerned, although the slope of ln σ_3 tends to increase for increasing N_A^0 (solid line). A linear fit of ln σ_3 versus $(N_A^0)^{-1/3}$ (dashed line) yields a proportionality factor of $-1.63\,\mathrm{nm}^{-1}$. This value should be of the order of magnitude of $-\alpha/a_h = -4.29\,\mathrm{nm}^{-1}$ (obtained for $\alpha = 1.73$, $a_h = 0.403$ nm), which is not very well obeyed. However, in view of the before-mentioned uncertainty in the value of m_h^*, a different value of a_h can be used. Taking the value of $m_h^* = 0.35 m_0$, obtained in the present study for sample HF-3(100), the resulting Bohr radius is $a_h = 0.864$ nm. This would give $-\alpha/a_h = -2.00\,\mathrm{nm}^{-1}$, which is in better agreement with the value of $-1.63\,\mathrm{nm}^{-1}$ obtained in figure 6.

It should be noted that in figure 6, we plotted the room temperature value of N_A^0 instead of the total boron concentration N_A. However, since at room temperature only a very small fraction of the acceptors is ionized and the compensation ratio is expected to be small, the two values will not differ much.

4.3. Nearest-neighbour versus variable-range hopping

For all diamond films, the conductivity values in the hopping region down to 110 K could fairly well be described by ln $\sigma \sim 1/T$ (see figure 5). However, when still lower temperatures are included (data available for the most heavily doped samples of runs HF-1 and HF-5) this linear relationship seems to be no longer valid, as is shown in figure 7. As was noted by Mott [27], conduction at sufficiently low temperatures only

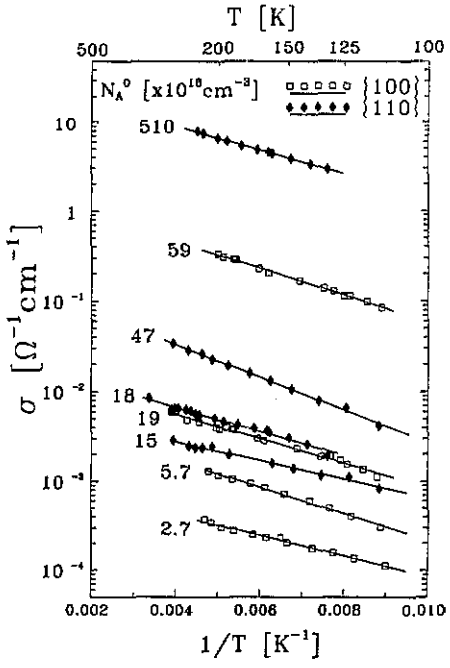

Figure 5. Data fitting of the conductivity in the hopping region down to 110K, showing the linear relationship between ln σ and $1/T$.

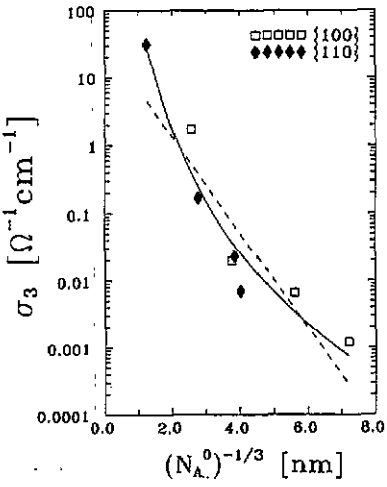

Figure 6. Pre-exponential factor σ_3 for hopping conductivity as a function of the inverse cubic root of the room temperature neutral boron concentration, $(N_A^0)^{-1/3}$. The dashed line represents a linear fit of ln σ_3 versus $(N_A^0)^{-1/3}$.

occurs between states within a very small band of energies near the Fermi level. As a result, hopping can take place between remote impurities whose energies happen to be within this band. This leads to variable-range hopping, as opposed to nearest-neighbour hopping at more elevated temperatures. Variable-range hopping has been shown to be proportional to $\exp(-T_0/T)^{1/4}$ [27]. In figures 7(*a*) and 7(*b*) we have plotted ln σ versus $1/T$ (lower x-axis) and versus $1/T^{1/4}$ (upper x-axis), for the runs HF-5 and HF-1, respectively. It is seen that a more or less linear relationship exists between ln σ and $1/T^{1/4}$, whereas for ln σ versus $1/T$ this is not the case. This indicates that the conduction mechanism at low temperatures could be variable-range hopping.

4.4. The connection with crystal growth

The higher conductivity values of {100} samples compared to {110} films in the band conduction region and the reversal in the hopping regime (see figure 1) can be explained on the basis of crystal growth theory. The growth mechanism for {100} diamond surfaces is essentially different from that for the {110} orientations. The {100} surfaces (which are F faces) are characterized by slow layer growth involving step and kink sites [28,29]. This leads to a relatively good crystallographic quality and low impurity content. At {110} surfaces (K/S faces), on the other hand, growth species are directly integrated into the lattice. Therefore, the growth velocity and also the impurity incorporation are much higher than for {100} surfaces. These views are

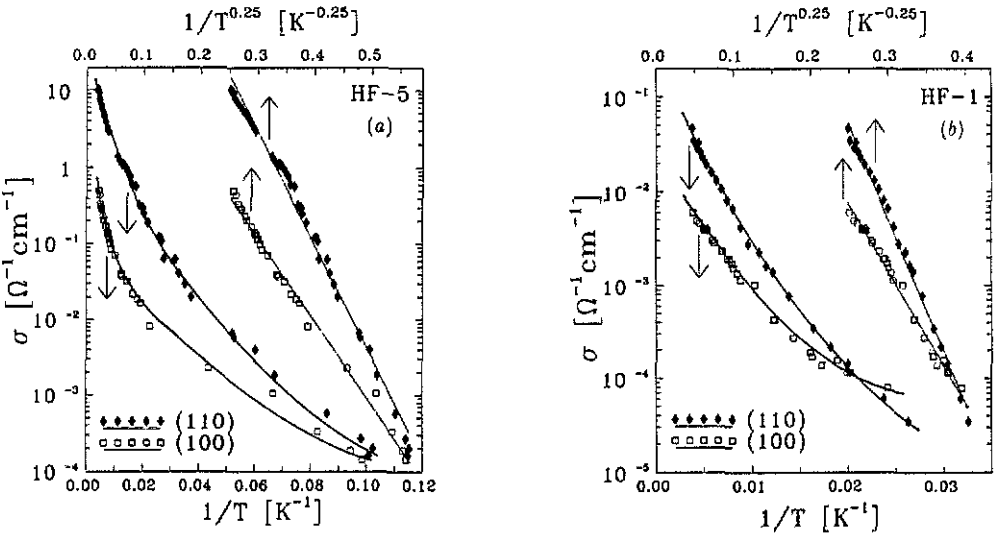

Figure 7. Low-temperature conductivity of the most heavily doped diamond films as a function of $1/T$ (lower x-axis) and of $1/T^{1/4}$ (upper x-axis); (*a*) run HF-5, (*b*) run HF-1.

in accordance with the data of table 1, which clearly show thinner layers and lower boron concentrations for {100} films compared to {110} layers.

The low-band conductivity of {110} films should thus be attributed to the lower carrier mobility, caused by the poorer crystallographic quality and higher impurity content as compared to {100} samples. This low mobility even overshadows the effect of the larger acceptor concentration in {110} films. Hopping conductivity, on the contrary, is not mobility controlled but depends on wave function overlap, which goes exponentially with $1/N_A^{1/3}$. Therefore, the higher hopping conductivity of {110} films is directly explained by their higher boron content.

4.5. Comparison with previously published results

The previously published results [5,7,8] on monocrystalline CVD diamond have all been obtained for temperatures above 200K. Accordingly, the authors have not observed a clear change in conduction mechanism, as in the present study.

Some interesting differences can be noted when our results are compared with those for the microwave-plasma-grown samples of Shiomi *et al* [5], where approximately the same range of doping levels was used. First, the change in electrical conductivity upon heat treatment, which had been attributed to diffusion of dissolved hydrogen in their films, was not observed in our case. Second, the reported 'metallic conduction' for their film with a dopant level of $3 \times 10^{20}\,cm^{-3}$ was not observed in any of our films. Even for our sample HF-5(110), with a neutral boron concentration of $5.1 \times 10^{20}\,cm^{-3}$, the conductivity was found to increase as a function of temperature. This may be due to the fact that the heavily doped sample of Shiomi *et al* is a (100)-oriented film, which should have a lower compensation ratio and a better crystallographic quality than our (110) sample. Since the Mott transition is shifted toward higher impurity concentrations for increasing compensation ratio [30],

the electrical conduction in sample HF-5(110) can still be activated, whereas that of [5] is already purely metallic. Finally, it should be noted that Shiomi *et al.* could not obtain proper theoretical fitting curves for their carrier concentration, unless they assumed the existence of additional acceptor-like centres in a concentration more than ten times larger than the boron concentration. However, in our view, this strange result might not have occurred if they had varied not only the compensating donor concentration in their fitting procedure, but also the value of the hole effective mass, which had been kept fixed at $m_h^* = 0.75m_0$.

Acknowledgments

The authors are grateful to Drukker International B V for offering the facility for metallization and laser cutting of the samples. Dr M Seal is gratefully acknowledged for his interest in the work and for critically reading the manuscript. Two of the authors (GJ and WV) acknowledge the Netherlands Technology Foundation (STW) for partial financial support.

References

[1] Mort J, Okumura K and Machonkin M 1991 *Phil. Mag.* B **63** 1031
[2] Muto Y, Sugino T and Shirafuji J 1991 *Appl. Phys. Lett.* **59** 843
[3] Sokolina G A, Bantsekov S V, Botev A A, Builov L L and Spitsyn B V 1988 *Izv. Akad. Nauk SSSR, Neorg. Mater.* **24** 1215
[4] Nishimura K, Das K and Glass J T 1991 *J. Appl. Phys.* **69** 3142
[5] Shiomi H, Nishibayashi Y and Fujimori N 1991 *Japan. J. Appl. Phys.* **30** 1363
[6] Narducci D, Guarnieri C R and Cuomo J J 1991 *J. Electrochem. Soc.* **138** 2446
[7] Fujimori N, Nakahata H and Imai T 1990 *Japan. J. Appl. Phys.* **29** 824
[8] Grot S A, Hatfield C W, Gildenblat G Sh, Badzian A R and Badzian T 1991 *Appl. Phys. Lett.* **58** 1542
[9] Janssen G, van Enckevort W J P, Vollenberg W and Giling L J 1992 *Diamond Relat. Mater.* **1** 789
[10] Chwang R, Smith B J and Crowell C R 1974 *Solid State Electron.* **17** 1217
[11] Shklovskii B I and Efros A L 1984 *Electronic Properties of Doped Semiconductors* (Berlin: Springer) ch 4
[12] Fritzsche H and Cuevas M 1960 *Phys. Rev.* **119** 1238
[13] Mansfield R, Abboudy S and Fozooni P 1988 *Phil Mag.* B **57** 777
[14] Collins A T and Williams A W S 1971 *J. Phys. C: Solid State Phys.* **4** 1789
[15] Blakemore J 1962 *Semiconductor Statistics* (New York: Pergamon)
[16] There is no sharply defined value of Na^3 for the onset of metallic conduction. Experimentally, the value of 0.02 is observed (see [11], p 253). However, a wide region of intermediate concentrations $0.02 < Na^3 < 1$ exists where conduction is no longer described by standard semiconductor statistics and is not yet of a fully metallic nature. For a more thorough treatment, see [11] part II, or
Mott N F and Davis E A 1971 *Electronic Processes in Non-Crystalline Materials* (Oxford: Clarendon) ch 5
[17] Mitchell E W J 1963 *Proc. 1st Int. Congress on Diamonds in Industry (Paris, 1962)* ed P Greene (London: Industrial Diamond Information Bureau) p 241
[18] Field J E 1979 *The Properties of Diamond* (London: Academic) p 653
[19] Janssen G, Vollenberg W, Giling L J, van Enckevort W J P, Schaminée J J and Seal M 1991 *Surf. Coat. Technol.* **47** 113
[20] Collins A T and Lightowlers E C 1979 *The Properties of Diamond* ed J E Field (London: Academic) p 86
[21] Massarani B, Bourgain J C and Chrenko R M 1978 *Phys. Rev.* B **17** 1758
[22] Baranskii P I, Torishnii V I and Chipenko G V 1988 *Sov. Phys.–Semicond.* **22** 1397

[23] Yamanouchi C 1965 *J. Phys. Soc. Japan* **20** 1029
[24] Williams A W S, Lightowlers E C and Collins A T 1970 *J. Phys. C: Solid State Phys.* **3** 1727
[25] Mott N F and Davis E A 1971 *Electronic Processes in Non-Crystalline Materials* (Oxford: Clarendon) pp 54, 175
[26] Shklovskii B I and Efros A L 1984 *Electronic Properties of Doped Semiconductors* (Berlin: Springer) ch 6
[27] Mott N F 1968 *J. Non-Cryst. Solids* **1** 1
[28] van Enckevort W J P, Janssen G and Giling L J 1991 *J. Cryst. Growth* **113** 295
[29] van Enckevort W J P 1991 *J. Hard Mater.* **1** 247
[30] Shklovskii B I and Efros A L 1984 *Electronic Properties of Doped Semiconductors* (Berlin: Springer) ch 13